EPJ Web of Conferences **290**, 01004 (2023) https://doi.org/10.1051/epjconf/202329001004
EuNPC 2022

Warsaw Active-Target TPC: a new detector for photonuclear reactions studies at astrophysical energies

Mikołaj Ćwiok[1,*], *Wojciech* Dominik[1], *Aleksandra* Fijałkowska[1], *Mateusz* Fila[1], *Zenon* Janas[1], *Artur* Kalinowski[1], *Krzysztof* Kierzkowski[1], *Magdalena* Kuich[1], *Chiara* Mazzocchi[1], *Wojciech* Okliński[1], *Piotr* Podlaski[1], *Marcin* Zaremba[1], *Moshe* Gai[2], *Sarah R.* Stern[2], *Deran K.* Schweitzer[2], and *Dimiter L.* Balabanski[3]

[1]Faculty of Physics, University of Warsaw, Poland
[2]LNS at Avery Point, University of Connecticut, CT, USA
[3]Extreme Light Infrastructure - Nuclear Physics, IFIN-HH, Magurele, Romania

Abstract. An active-target time-projection chamber (TPC) optimised for studying nuclear reactions of astrophysical interest was developed by the University of Warsaw for studying photo-disintegration reactions using intense, monochromatic γ-ray beams. Different reactions can be studied by tuning composition and density of the gaseous target for particular energy of the gamma beam. The Warsaw TPC detector, with its active volume of about $33\times20\times20\,\mathrm{cm}^3$ centred around the beam axis and micro-pattern structures (GEMs) employed to amplify the primary ionisation induced by charged particles produced in reactions in the gaseous target, is characterised by a readout based on signal strips, arranged into 3-coordinate redundant system. The 3D kinematics of charged particles in the event are reconstructed from a total of about 10^3 channels read out by digitising front-end electronics based on the General Electronics for TPCs (GET). In this paper the principles of detector operation and basic track reconstruction methods are discussed and illustrated by means of preliminary results from pilot measurements conducted in 2021-22.

1 Introduction

Modelling of the process that govern stars evolution requires as input, among others, the reaction rate per particle pair for the thermonuclear reactions that take place in the stars core. These rates are energy (temperature) dependent and directly proportional to the reaction cross section, which decreases exponentially with decreasing energy. The cross section has to be measured at the same energies at which the reactions happen in the stars (i.e. at the so-called Gamow peak) [1]. Since the relevant energies are well below the Coulomb barrier, these thermonuclear reactions are characterised by extremely low cross sections, often beyond the reach of modern-day experiments. Typically, experimental knowledge is gathered for as low energies as possibly achieved and extrapolations by means of R-matrix models are employed to extrapolate the cross section at the Gamow peak. It is therefore necessary to measure the cross section for astrophysically-relevant reactions at as low energies and as accurately as possible in order to constrain the R-matrix fit. Among the most important reactions that take place in the core of a star are direct-capture reactions, namely (α,γ) and (p,γ). From the experimental point of view, the tiny rates that characterise these reactions can be increased significantly by taking advantage of the principle of detailed balance [2]. One of the key problems in nucleosynthesis is how to understand or explain the ratio between oxygen and carbon in the Universe. This ratio is governed by one reaction in particular, $^{12}\mathrm{C}(\alpha,\gamma)^{16}\mathrm{O}$, at centre-of-mass energies below $\sim$2 MeV, with the Gamow peak for helium-burning temperatures being at $\sim$300 keV.

In this work, cross sections for nuclear reactions at astrophysical energies are studied by means of the inverse photo-disintegration reactions, with the flagship being $^{16}\mathrm{O}(\gamma,\alpha)^{12}\mathrm{C}$. The goal is to investigate it at the lowest possible energies, i.e. to about 1 MeV in the centre-of-mass. For this purpose, intense, monochromatic γ ray beams are needed, as well as a detection system able to measure the momenta of the charged reaction products. In comparison with direct capture measurements the reactions induced by γ-rays are characterised by inherently low experimental backgrounds, different systematic uncertainties and larger cross sections due to detailed balance principle of nuclear reactions.

An active-target Time Projection Chamber (TPC) detection technique is employed for momenta measurements and particle identification. In TPCs of this kind a gaseous active volume acts as both the target for nuclear reactions and as the medium for charge transport and amplification. Nowadays active target detectors with tracking capabilities of low-energy charged particles are adopted in more than a dozen experiments in nuclear and particle physics [3–5].

The Warsaw TPC detector was specifically designed to operate with lower-than-atmospheric gas pressures and is optimised for studying reactions induced by narrow neutral beams, such as γ-rays and neutrons. The experimental

*e-mail: Mikolaj.Cwiok@fuw.edu.pl

technique presented in this work results from a decade-long R&D programme carried out by the University of Warsaw (UW) in collaboration with the University of Connecticut, CT, USA and the Extreme Light Infrastructure Nuclear Physics / IFIN-HH, Bucharest-Magurele, Romania, to build and use in experiment a full-scale demonstrator of the TPC dedicated to ELI-NP [6–8].

2 Detector and data acquisition system

The apparatus consists of a low-pressure vessel, an internal TPC structure and external front-end electronics attached on top of the vessel (see Figure 1).

The internal detector structure is composed of: a drift cage, micro-pattern amplification structures and a segmented readout anode (see Figure 2). The electron drift cage consists of: a 4 mm-thick cathode plate made of aluminium and 12 field shaping 2 mm-thick aluminium electrodes having 16 mm pitch, for a total drift length of 196 mm, and with uniformity of the drift electric field better than 1% in the entire active volume. Primary ionisation charge is amplified by a stack of three 50 μm-thick Gas Electron Multiplier (GEM) foils [9] interlaced with 3 mm-wide transfer gaps. The induced signals are collected by a segmented multi-layer PCB anode. The active area is a $330 \times 200\,\mathrm{mm}^2$ rectangle with chamfered corners at 30° and consists of many tessellated diamond-shaped gold-plated pads (1 mm edge, *Via in Pad* technology). The pads are arranged along three main axes at 60° with respect to each other, and which form three independent linear sets of strips (U, V, W) with 1.5 mm pitch (see insert in Figure 2). Such a redundant planar 3-coordinate system allows for unambiguous creation of virtual pixels on a 2D plane for a given instant of time provided that measured track topologies are relatively simple, e.g. several straight tracks in a single recorded event. Most of the strips are split in half and read out by two independent electronic channels in order to further reduce ambiguity for more complex event topologies. The U-strips are parallel to the nominal gamma beam trajectory. In total 1018 electronics channels are being read out: 264 for U, 376 for V and 378 for W strips, respectively. The third cartesian coordinate along the drift electric field, $\vec{E}_{\mathrm{drift}}$, is determined from drift time assuming known electron drift velocity.

The TPC internal structure is immersed in a stainless steel vacuum vessel of 170 dm^3 volume with horizontally-oriented UVW readout PCB. The top lid and side walls of the vessel are equipped with several vacuum ports for installing high voltage and analogue signal feedthroughs, gamma beam windows and radioactive calibration sources. The vessel is connected to a low-pressure gas system consisting of: a high-pressure gas cylinder with a double-stage pressure regulator, an upstream mass-flow controller unit, two precise gas dosing valves at inlet and outlet ports, a set of vacuum and pressure gauges, a programmable Proportional-Integral-Derivative (PID) pressure control unit, a downstream dry four-stage diaphragm pump and a turbo-molecular pump. After initial evacuation of the vessel down to vacuum levels of 10^{-5} – 10^{-4} mbar, the detector is operated in an open loop flow mode with gas exchange rates varying between 1 and 4 detector volumes per day.

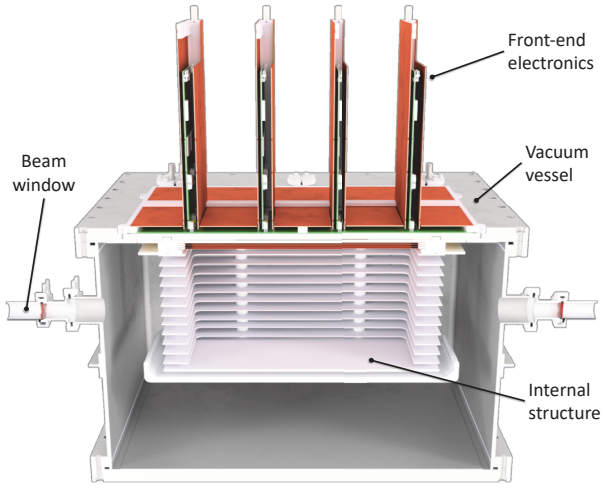

Figure 1. Half-section view of the Warsaw TPC detector.

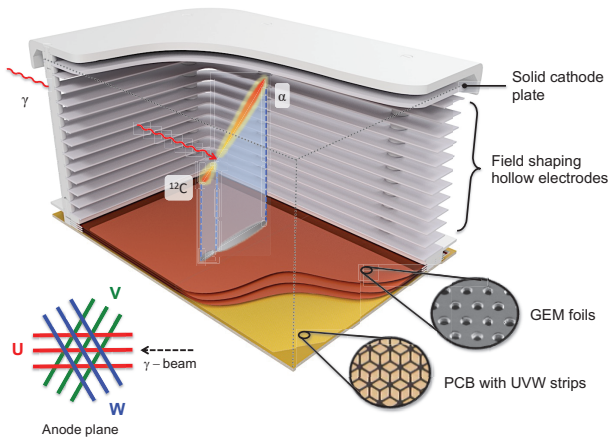

Figure 2. Details of internal structure of the Warsaw TPC with superimposed artistic rendering of ^{16}O photo-disintegration event. The concept of UVW readout strips is illustrated in the bottom-left insert.

The data acquisition (DAQ) system is based on the General Electronics for TPCs (GET) [10]. Analogue signals from the readout anode are extracted via 4 vacuum feedthroughs and routed to 4 commercial *ASIC and ADC* (AsAd) front-end cards equipped with custom-designed protection boards and electromagnetic shielding. Each AsAd card contains 4 *ASIC for GET* (AGET) chips with 64 active channels and 4 blinded channels for evaluating characteristic fixed-pattern noise. Inside each AGET chip signals undergo amplification and shaping stages, which are followed by a Switched Capacitor Array (SCA) acting as an analogue memory buffer with 512 time cells. Signal sampling frequency can be adjusted from 1 to 100 MS/s (in 7 steps), dynamic range from 120 fC to 10 pC (in 4 steps) and characteristic shaping time from 70 ns to 1 μs (in 16 steps). Upon receiving the event accept signal all stored charges are digitised by a 12-bit ADC and transmitted outside of the AsAd board to the main 1024-channel DAQ

module for further processing. This module, referred as *z-CoBo*, was custom-designed and built at the Faculty of Physics, UW. It employs *System on Chip* architecture that combines the Field Programmable Gate Array (FPGA) part and the Hard Processor System (HPS) part in a single Xilinx Zynq-7045 chip. This novel solution offers similar functionality to the original Concentrator Board (CoBo) of GET electronics, which was based on the legacy Xilinx Virtex-5 chip. The DAQ module also provides event time-stamping and optional high-level triggering. The raw-data are transmitted by one (or more) 1 Gbit/s Ethernet link(s) from the z-CoBo to a dedicated DAQ server PC and then to a Network Attached Storage disk matrix. The maximal sustained trigger rate is limited to 80 Hz for a single Ethernet link and without zero-suppression of the data.

In case of semi-continuous beams or radioactive calibration sources the Warsaw TPC is operated in self-trigger mode, in which a collective analogue signal from the last GEM amplification stage is routed to the fast NIM electronics for further amplification, shaping and discrimination in order to form a 100 μs-wide gate signal for the DAQ module. The acquisition is then stopped after certain programmable delay so that the arrival time of the first charged particle track corresponds to 10% of the full time scale. In this mode the position of a track along detector's axis parallel to the drift electric field is determined only up to an additive constant. The discriminator's threshold is adjusted for a given TPC high-voltage working point for efficient detection of particles of the reaction of interest.

A dedicated Detector Control System (DCS) software framework allows for remote operation of the apparatus, including: setting TPC high-voltage working points, changing working gas pressure and periodical recording of various working conditions, such as: gas flow, pressures, voltages, currents and temperatures [11].

3 Experimental setup

The detector was assembled at the Faculty of Physics, UW in 2020. It was initially commissioned with two collimated ^{241}Am radioactive sources installed in close proximity to the active volume, namely: the first one located 6 mm behind the cathode plate and emitting α-particles parallel to $\vec{E}_{\mathrm{drift}}$ through a tiny hole, and the second one located on the side, about 73 mm away from the active volume, that emitted α-particles perpendicular to $\vec{E}_{\mathrm{drift}}$. These calibration measurements with weak radioactive sources allowed us to validate simulations of electron drift velocity and particle ranges.

The first measurement with a gamma beam was conducted in June 2021 at the Van der Graaf accelerator at the Institute of Nuclear Physics, Polish Academy of Sciences (IFJ-PAN), Cracow, Poland. In this experiment 13 MeV gamma photons were created in the ^{15}N(p, γ)^{16}O reaction by bombarding ^{15}NCr target deposited on a tantalum backing with a 1.03 MeV proton beam. The resulting gamma beam was shaped by means of a lead absorber inserted between the solid target and the brass beam entrance window to illuminate only the middle part of the drift cage. The detector was operated with a pure CO_2 gas kept at 250 mbar absolute pressure. Candidate events for ^{16}O(γ, p)^{15}N and ^{16}O(γ, α)^{12}C reactions were clearly observed [12].

Between April and September 2022 the second ^{16}O and ^{12}C photo-disintegration experiment was conducted at the High Intensity γ-Ray Source (HIγS) facility at the Triangle University Nuclear Laboratory (TUNL), Durham, NC, USA [13]. The γ-rays were produced in Compton back-scattering of a free-electron laser beam with a relativistic electron beam. A lead collimator with 10.5 mm aperture located about 60 m away from the γ production point provided almost collinear beam that fit inside the 14 mm-wide gap between two adjacent field shaping electrodes in the middle plane of the TPC drift cage. The detector was equipped with Kapton windows of 25 mm diameter at beam entrance and exit ports (50 μm and 125 μm-thick, respectively).

The TPC vessel was aligned using a dedicated visible laser beam that was collinear with the nominal gamma beam trajectory. A refined detector alignment was done with the gamma beam using a set of lead plugs placed in front and rear ports of the detector and a gamma camera located downstream of the TPC vessel. The remaining residual beam tilt and offset are determined for each beam energy in the offline analysis step on the basis of vertex distribution on the UVW readout plane for candidate photo-disintegration events.

In total 15 beam energy points were measured during 275 h of the allocated beam time, ranging from 8.51 MeV to 13.9 MeV (nominal E_{CM} from 1.35 MeV to 6.7 MeV for ^{12}C(α, γ) reaction, respectively) [2]. For each energy the TPC operating conditions were optimised for charged particle ranges in detector's active volume. In particular, three pressure settings of pure CO_2 gaseous target were used during the measurements: 130, 190 and 250 mbar. The readout electronics was operated with: dynamic range of 120 fC, characteristic shaping time of 232 ns and two settings of the sampling frequency: 12.5 MHz or 25 MHz.

During data-taking the relative beam intensity was constantly monitored by a set of scintillation counters positioned before the TPC. For most of the scanned energy points the (γ, n) activation measurements of thin ^{197}Au discs placed at the exit window of the TPC were performed in order to determine absolute photon fluxes and to establish correlation with the scintillator-based method. For one beam energy a small photo-fission ionisation chamber with ^{238}U target was used at the rear TPC window as an alternative method to measure the absolute photon flux over time. Preliminary analysis of partial data yields beam intensities between $1 \cdot 10^8$ γ/s and $5 \cdot 10^8$ γ/s depending on the beam energy. The energy spectra of γ-rays were measured at 8-20 h intervals by means of a high-purity germanium detector located behind the TPC. The FWHM energy spread for the lowest studied energy point of E_γ=8.51 MeV was about 350 keV.

4 Event selection and reconstruction

All recorded raw-data waveforms were corrected for pedestals of individual electronic channels and for fixed-pattern-noise shape common for 64 channels of a given

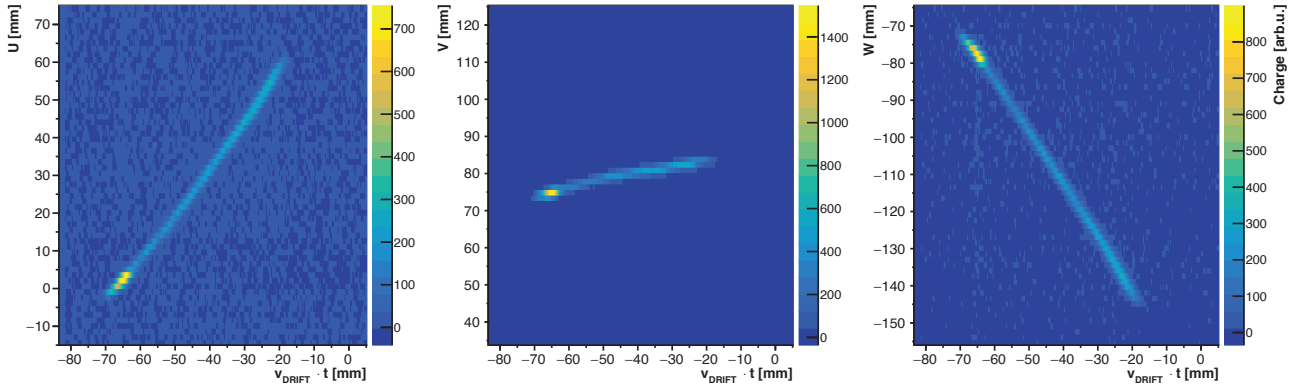

Figure 3. Example of a ^{16}O photo-disintegration candidate event collected at E_γ=13.9 MeV. Positions in strips on the anode plane and time bins along the drift direction are represented in millimetres assuming known strip pitch and electron drift velocity. A 90 mm × 90 mm region of interest is enlarged for each of U, V and W projections (p=250 mbar, 12.5 MHz sampling rate).

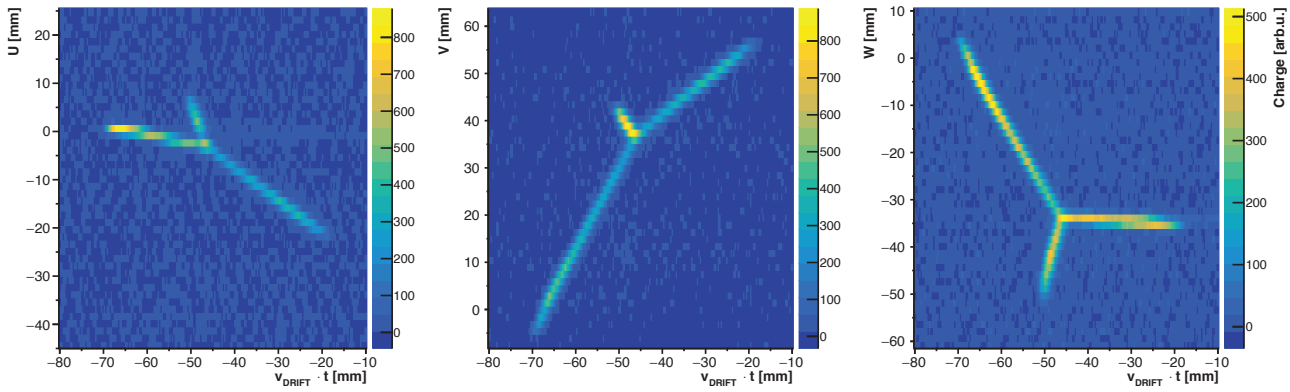

Figure 4. Example of a ^{12}C photo-disintegration candidate event collected at E_γ=13.9 MeV. Positions in strips on the anode plane and time bins along the drift direction are represented in millimetres assuming known strip pitch and electron drift velocity. A 70 mm × 70 mm region of interest is enlarged for each of U, V and W projections (p=250 mbar, 12.5 MHz sampling rate).

AGET chip in the front-end electronics. Afterwards 2D charge distributions of strip position vs. drift length were created separately for U, V and W strip arrays. Such distributions were visually inspected and collected events were assigned to categories according to their respective topology: 2- and 3-particles, background/noise. In Figures 3 and 4 the raw-data distributions from U, V and W strip arrays are depicted for a typical event from 2- and 3-particle category, respectively.

Background consisted of α particles from radon generated in the decay of ^{232}Th and ^{238}U isotopes that are present in welded seams of the vacuum vessel (amounting to ~0.15 Hz in total trigger rate), and of recoils following beam-induced (γ, n) reactions on the nuclei of CO_2 molecules. Such events appear as long bright tracks and short bright tracks ("dots"), respectively, and they are easily separated from the remaining events. Those events classified as 2- or 3-particles were analysed further to apply detector fiducial cuts and to determine the momenta of the particles in 3D. The fiducial cuts ensured that: (i) positions of the vertices on the UVW plane were inside a band defined by the gamma beam collimator with 2 mm safety margin; (ii) positions of the endpoints of all tracks were fully contained within the UVW active area with 5 mm safety margin; (iii) tracks were fully contained within the SCA memory buffer with a safety margin of at least 2 time cells; (iv) tracks did not interfere with the first 25 time cells of the SCA memory buffer used for calculating pedestals on event-by-event basis. Last but not least, the rate of observed pile-up effects with more than one gamma interaction in the same event was negligible.

Due to the presence of natural isotopes of oxygen and carbon in the CO_2 gaseous target, the 2-particle event category also contains admixture of $^{17,18}\mathrm{O}(\gamma,\alpha)^{13,14}\mathrm{C}$, $^{16}\mathrm{O}(\gamma,\mathrm{p})^{15}\mathrm{N}$ and $^{13}\mathrm{C}(\gamma,\alpha)^{9}\mathrm{Be}$ reactions. Such an isotopic contaminant background can be discriminated based on reaction Q-values. Separation energies for beam-induced background reactions relevant to the studied energy range are listed in Table 1. The 3-particle event category contains triple-alpha final states stemming from $^{12}\mathrm{C}(\gamma, 3\alpha)$ reaction.

Two methods of track finding were used for preliminary analysis presented in this paper. The first one is based on human-based determination of track segments and the second one on automatic reconstruction, which is currently optimised only for identifying 2-particle events with back-to-back topology. In case of automatic procedure the charge deposits, *hits*, are grouped into clusters

around *seed hits* that passed certain threshold level. The clustered hits are used to find the *approximate axis* of a 2-particle event in 3D space based on three 2D projections from U, V and W strip arrays. Afterwards all clustered hits are projected onto this approximate axis to form a 1D charge distribution. The resulting distribution is then fitted for a given reaction hypothesis with the sum of two templates of energy loss along the track, dE/dx, in order to fine-tune endpoints of the tracks and position of the common vertex in 3D space (see Figure 5). In the final step a parameterised dependence of the average range as a function of the kinetic energy for a given isotope and gas density is employed to determine scalar momenta of the particles. The dE/dx templates and particle ranges are obtained from Monte Carlo simulations [15, 16]. In order to overcome imperfections of the modelling of particles' ranges we plan to fine-tune the absolute energy scale *in situ* using known resonances in ^{16}O for the studied energy range, namely: a narrow 2^+ resonance at excitation energy of 9.845 MeV and three broader ones at excitation energies of 11.51 MeV (2^+), 12.45 MeV (1^-) and 13.09 MeV (1^-) [17].

5 Preliminary results

In this paper we present preliminary results from partial statistics of the collected data sample during the HIγS experiment, which demonstrate various technical capabilities of the Warsaw TPC, such as discriminating between reaction channels and measuring angular distributions. The beam enters the detector horizontally parallel to the anode plane and perpendicular to the $\vec{E}_{\text{drift}}$ vector (vertical). The coordinate system origin is the centre of the TPC drift cage. For momenta representation, a spherical coordinate system (BEAM) is used, with Z axis parallel to the beam, and with θ and ϕ being the polar and azimuthal angles, respectively. Assignment of the 2-particle event to the ^{16}O$(\gamma,\alpha)^{12}$C or to the ^{17,18}O$(\gamma,\alpha)^{13,14}$C reactions can be done by comparing the track lengths, since the reactions have Q-values that differ by about 1 MeV (see Table 1). In Figure 6 the histogram of the sum of measured α and carbon track lengths is shown for E$_\gamma$=8.66 MeV. The group of events below 50 mm corresponds to the ^{16}O$(\gamma,\alpha)^{12}$C decay channel, while the group of events above this threshold to the ^{17,18}O$(\gamma,\alpha)^{13,14}$C. It can be seen that the ^{16}O(γ,α) decay channel is well distinguished from the background reactions that dominate the rate of measured 2-particle events at this γ beam energy.

The angular distributions of particles emitted in the reactions can be reconstructed as well and used to improve reaction identification. An example of two-dimensional selection cuts for ^{16}O photo-disintegration candidates at E$_\gamma$=11.5 MeV is shown in Figure 7, in which the track length of the α particle is plotted as a function of cosine of the polar angle θ in the laboratory reference frame. Events corresponding to ^{16}O(γ,α) decay channel are contained in-

Table 1. Separation energies in MeV for: neutrons, protons and alpha particles in ^{12,13}C and ^{16,17,18}O isotopes [14].

	^{12}C	^{13}C	^{16}O	^{17}O	^{18}O
S_n	18.722	4.946	15.664	4.144	8.044
S_p	15.957	17.533	12.127	13.780	15.942
S_α	7.367	10.648	7.162	6.359	6.227

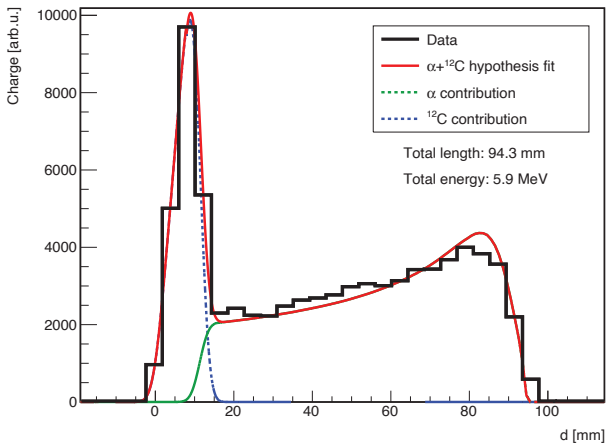

Figure 5. Fitted $\frac{dE}{dx}$ templates superimposed on the observed charge distributions along candidate tracks for 2-particle event shown in Figure 3 (E$_\gamma$=13.9 MeV, p=250 mbar, automatic reconstruction).

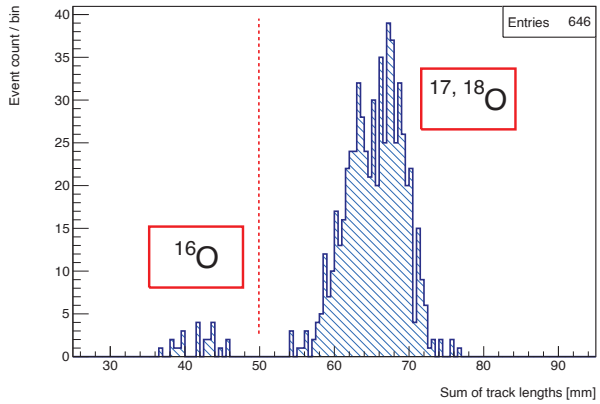

Figure 6. Example of 1D identification plot based on the sum of α and carbon track lengths (E$_\gamma$=8.66 MeV, p=130 mbar, manual reconstruction, partial statistics).

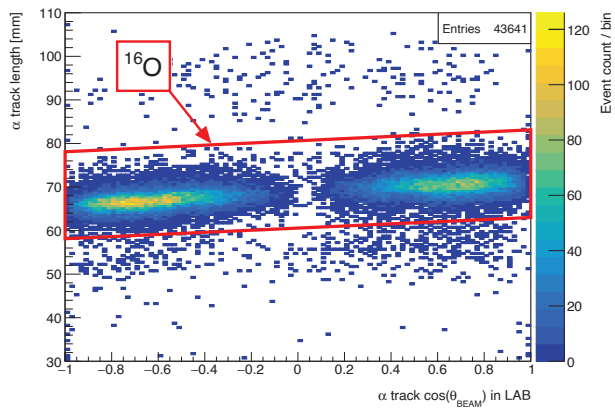

Figure 7. Example of 2D identification plot based on α-particle track length and its cosine of the polar angle θ (E$_\gamma$=11.5 MeV, p=190 mbar, automatic reconstruction, LAB reference frame).

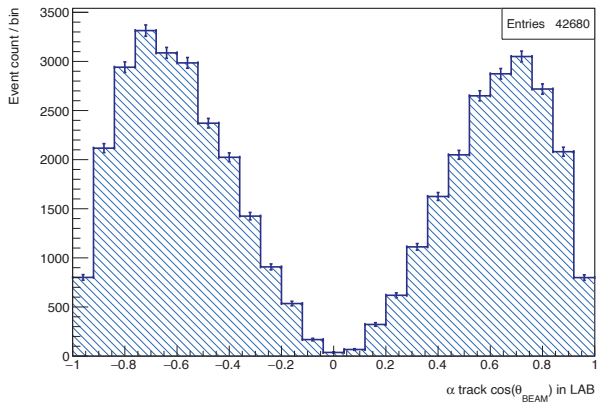

Figure 8. Distribution of cosine of the polar angle θ of α particles from $^{16}O(\gamma,\alpha)^{12}C$ candidate events after selection cuts shown in Figure 7 (E_γ=11.5 MeV, p=190 mbar, automatic reconstruction, LAB reference frame).

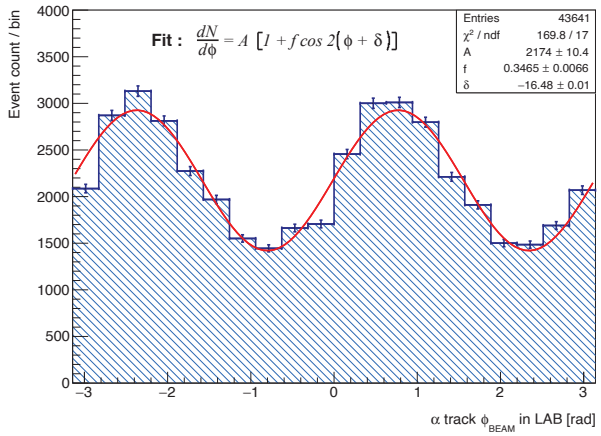

Figure 9. Distribution of azimuthal angle ϕ of α particles in 2-particle event category. The fit equation and parameters are shown in the figure (E_γ=11.5 MeV, p=190 mbar, automatic reconstruction, LAB reference frame).

side the indicated selection band. Such a cut results in better purity than the one based on α-particle track length alone. In Figure 8 the resulting distribution of cosine of the polar angle θ is shown for events tagged as $^{16}O(\gamma,\alpha)$ using 2D selection cut from Figure 7. The characteristic shape of E2 multipolarity can be observed as expected for the 2^+ resonance in ^{16}O at the excitation energy of 11.51 MeV [17].

The distributions of the azimuthal angle ϕ were used to characterise the gamma beam delivered to the TPC detector. An example of such distribution from the reconstructed momenta of 2-particle events is depicted in Figure 9 for E_γ=11.5 MeV. The observed shape corresponds to a gamma beam circularly polarised more than 90%, as expected from independent measurements of the polarisation of the laser beam [18].

6 Summary and outlooks

At the University of Warsaw an R&D program to design and construct active target time-projection chambers optimised for reactions induced by neutral beam (γ-rays and neutrons) has been developed over the last 10 years. The physics goals driving the project consist in the study of nuclear reactions of astrophysical interest at the relevant energies. The main features characterising the detector are illustrated as well as data processing. The first experiments with the full-scale demonstrator were conducted in 2021 and 2022 at IFJ-PAN, Cracow, Poland and HIγS at TUNL, Durham, NC, USA, respectively. The highlight of the experiments was the study of the $^{16}O(\gamma,\alpha)^{12}C$ reaction at energies below 2 MeV in the centre-of-mass. Full statistics of the collected data is under evaluation. New experiments are planned at HIγS and ELI-NP facilities after 2024 to explore even lower centre-of-mass regions using γ-ray beams of higher intensity.

The authors would like to thank the staffs of HIγS and IFJ-PAN for providing high-quality beams during the experiments, as well as engineers H. Czyrkowski and R. Dąbrowski (UW) for their excellent technical support. This scientific work is supported by the National Science Centre, Poland (contract no. UMO-2019/33/B/ST2/02176), by the University of Warsaw, Poland (Interdisciplinary Centre for Mathematical and Computational Modelling – computational allocation no. G89-1286 and Excellence Initiative Research University – IDUB program), by the US Department of Energy, Office of Science, Office of Nuclear Physics (grant no. DE-FG02-94ER40870) and by the Romanian Ministry of Research, Innovation and Digitalization (contract no. PN 23.21.01.06).

References

[1] W.A Fowler, Rev. Mod. Phys. **56**, 149 (1984)
[2] M. Ćwiok *et al.*, EPJ Web Conf. **279**, 04002 (2023)
[3] D. Bazin *et al.*, Progress in Particle and Nucl. Phys. **114**, 103790 (2020)
[4] P. Egelhof *et al.*, ACTAF TDR, FAIR/GSI (2016)
[5] B. Adams *et al.*, arXiv:1808.00848 [hep-ex]
[6] M. Ćwiok, Acta Phys. Pol. B **47**, 707 (2016)
[7] O. Tesileanu *et al.*, Romanian Rep. Phys. (Suppl.) **68**, S699 (2016)
[8] M. Ćwiok *et al.*, Acta Phys. Pol. B **49**, 509 (2018)
[9] F. Sauli, Nucl. Inst. and Methods A **386**, 531 (1997)
[10] E.C. Pollacco *et al.*, Nucl. Inst. and Methods A **887**, 81 (2018)
[11] M. Fila, PhD thesis, Univ. of Warsaw (in preparation)
[12] M. Kuich *et al.*, Acta Phys. Pol. B (Proc. Suppl.) **16**, 4-A17 (2023)
[13] H.R. Weller *et al.*, Progress in Particle and Nucl. Phys. **62**, 257 (2009)
[14] M. Wang *et al.*, Chin. Phys. C **45**, 030003 (2020)
[15] J.F. Ziegler, M.D. Ziegler and J.P. Biersack, Nucl. Inst. and Methods B **268**, 1818 (2010)
[16] J. Allison *et al.*, IEEE Trans. Nucl. Sci. **53**, 270 (2006)
[17] R.J. deBoer *et al.*, Rev. Mod. Phys. **89**, 035007 (2017)
[18] Y.K. Wu, priv. comm. (2022)